International Journal of Advanced Research and Review

www.ijarr.in

EFFECT OF AL DOPING ON STRUCTURAL, OPTICAL, ELECTRICAL AND PHOTO-CATALYTIC PROPERTIES OF CUO NANOPARTICLES

S.Muthukrishnan[*], Venkat subramaniam[1], T.Mahalingam[2], S.J.Helen[3], P.Sumathi[4]

[1]Department of Electronics, PSG College of Arts and Science, Coimbatore-641014, India
[2]Department of Physics, Alagappa University, Karaikudi -630003, India
[3]Department of Physics, Karunya University, Coimbatore-641114, India
[4]Department of Physics, Rathinam Institutions, Coimbatore-641021, India
Corresponding author:*S.Muthukrishnan, Research Scholar, Department of Electronics, PSG College of Arts and Science, Coimbatore-641014, India. **Email:**s.muthukrishnan@rediffmail.com

ABSTRACT

Pure and Al doped CuO thin films were coated on glass substrate at 400°C by spray pyrolysis method for various aluminium concentrations (0%,1%, 2% and3%). Undoped and Al doped CuO thin films were characterized by various techniques such as X-ray diffraction, SEM, EDAX, UV-visible spectroscopy, FTIR, Hall measurements and Antibacterial activity.XRD diffraction patterns reveal that the films are polycrystalline in nature exhibiting monoclinic crystal phase structure. The prominent peak corresponds to (111) plane and the corresponding calculated crystallite size varies from 2 to 7 nm. SEM images show that the films exhibit grains of uniform size which are agglomerated for films with higher dopant concentration. It is found that the optical transmittance decreases with the increase in Al concentration and good optical energy band gapvariation was observed from 2.38 to 2.48eV for various Al doping concentration levels. The main reflection of this mineral could not be detected at these temperatures by the XRD but due to the higher sensitivity of FTIR technique this identification is possible. Electrical studies done using Hall measurement system exhibit that the undoped and Al doped CuO films are p-type semiconductors with carrier concentration in the order of $10^{14}cm^{-3}$. The electrical resistivity of the Al: CuO films ranges from 4.701×10^{-3} to 6.952×10^{-3} Ωcm. Also additionally anti-bacterial activity the films were investigated using microbial study which showed desirable bioactivity on the thin films.

KEYWORDS: XRD, Optical, Electrical, Antibacterial

1 INTRODUCTION

Transparent conducting oxides (TCOs) gain momentum in semiconductor technology due to their low cost and high performance (I.Akyuz et al., 2010). The development of semiconductor thin films is one of the key technologies for p-n junction based devices such as diode, transistors, and light emitting diodes transistors, and light emitting diodes. Cupric oxide (CuO), a semiconductor has several unique features such as low-cost, non-toxicity, abundant availability in the form of copper, 19% theoretical solar cell efficiency and relatively simple to form oxide layer, etc. (Reddy KTR et al., 2003).In order to utilize CuO for electrochemical and photoelectrochemical applications, it needs to be prepared as nanostructured thin films. Thin films of cupric oxide have been prepared by a number of techniques including pulsed laser deposition (Kim et al., 2003), thermal oxidation (Zhao et al., 2002), CuO films are used in the fabrication of optoelectronic devices such as photo transistors, photo diodes and transparent electrodes in flat-panel displays. It finds its application in liquid crystal displays, IR detectors and anti-reflection coatings (Ilican.S et al., 2009). Further, it is a suitable candidate for a window layer on CuO hetero junction solar cells (Kumaravel.R et al., 2010). As the sensitivity

and electrical conductivity of the CuO films are consistent, they are used in liquefied gas sensors.

The search for novel materials offering high performance with the ease of preparation at lower cost is always essential for today's technology. Non stoichiometric undoped CuO thin films usually exhibit low resistivity due to native defects of oxygen vacancies and cadmium interstitials. Therefore, resistivity of the films can be improved by controlling these native defects. In order to control the electrical and optical properties of CuO films, the type and properties of doped ions play a crucial role. Bulk CuO has an energy band gap of 2.5 eV which offers poor optical transparency in the short wavelength range of the visible spectra. A divalent metal doping offers the possibility of tuning the electronic and optical band gap to a carrier concentration dependent Burstein-Moss energy level shift (Kumaravel.R et al., 2012). It is found that when some metallic ions like Sn, In and Al processing smaller radius than Cu^{2+} (0.137 nm) doped in CuO films improve its electrical conductivity and change its optical energy band gap (Metz.A.W et al., 2004).

CuO thin films could be synthesized by various techniques such as sol-gel spin coating (Ilican.Z et al., 2002), dip coating (Murali.K.R et al., 2010), pulsed laser deposition (Gupta.R.K et al., 2009), metal-organic chemical vapour deposition (MOCVD) (Metz.A.W et al., 2004), thermal evaporation (Wongcharoen.N et al., 2012) and chemical bath deposition (Mane.S et al., 2000). The spray pyrolysis technique has a few advantages when compared with other methods. It is simple, basic set-up is not expensive, flexible for process modifications and is used for the preparation of a large number of semiconducting and insulating thin films (Bhosale.C.H et al., 2005). In the present work, we have prepared Al: CuO films by spray pyrolysis method and investigated the properties using various characterization tools. Moreover, in order to enhance the conductivity, we have chosen the dopant material as aluminium with various dopant concentrations from 1 to 3 % and systematically studied the change in behaviour of Al: CuO thin films using structural, optical and electrical characterization techniques.

2 EXPERIMENTAL DETAILS

Copper acetate was dissolved in distilled water at room temperature and water was used as solvent to synthesize CuO thin films using spray pyrolysis technique. Aluminium chloride anhydrous ($Al(Cl_3)_3.9H_2O$) was the source for aluminium doping and the concentration of the dopant was varied as 0,1, 2 and 3 wt%. Well cleaned glass substrates were placed on the heater and a distance of 18 cm was maintained between the tip of the nozzle and surface of the substrate. A constant flow rate, 3ml/min has been chosen for all films which would be sprayed on substrates kept at a temperature of 400°C. Before supplying the compressed air, the heater was followed to heat the substrate to attain the required temperature. When compressed air along with the precursor solution was passed through the nozzle at constant pressure, finely formed aerosol descended to reach the reactor zone where the film was deposited on the heated substrate. The possible chemical reactions that take place on the heated substrate to produce CuO and Al: CuO films may be as follows (Khan.M.K.R et al., 2010):

$$(CH_3COO)_2Cu.H_2O \xrightarrow{\text{decomposed at 400°C}} CuO + CO_2\uparrow + CH_4\uparrow + \text{steam}\uparrow$$

$$(CH_3COO)_2 + Al(Al(Cl_3)_3.9H_2O + H_2O \xrightarrow{\text{decomposed at 400°C}} Al: CuO + NO\uparrow + CO_2\uparrow + CH_4 + \text{steam}\uparrow$$

X-ray diffraction analysis was performed using X ray diffractometer (Shimadzu X-600) in order to study the crystal structure of the spray pyrolysed thin films. The surface morphology was recorded using scanning electron microscope (SEM, JOEL 2-JSM 6000). Optical transmission spectra of all the deposited films were obtained using UV-VIS spectrophotometer (UV Vis NIR Jasco V-670). The electrical studies were carried out using Hall measurement system (D.O.No.SR/S2/CMP-35/2004).

3 RESULTS AND DISCUSSION

The spray pyrolysed thin films were smooth, well adherent and visually transparent. Figure 1 shows the X-ray diffraction patterns for doped and Al: CuO thin films coated on glass substrates at 400°C.

These films show a preferential growth along the (200) diffraction and the other peaks associated with the (111), (200) and (202) planes are also observed. The characteristics peaks at 2θ =23.96°, 35.55° and 38.81° are identified from JCPDS card no. 65-1228 corresponding to the cubic structure of CuO: Al thin films (Table 1). It is observed that the preferential diffraction peak from (111) plane shows increase in intensity as the dopant concentration increases. The determined lattice constant for the dominant peak of CuO is found to be a = 0.137 nm which is well consistent with the reported value, 0.138 nm (Khan.M.K.R et al). The crystallite size of the sample is determined using the Scherrer's formula,

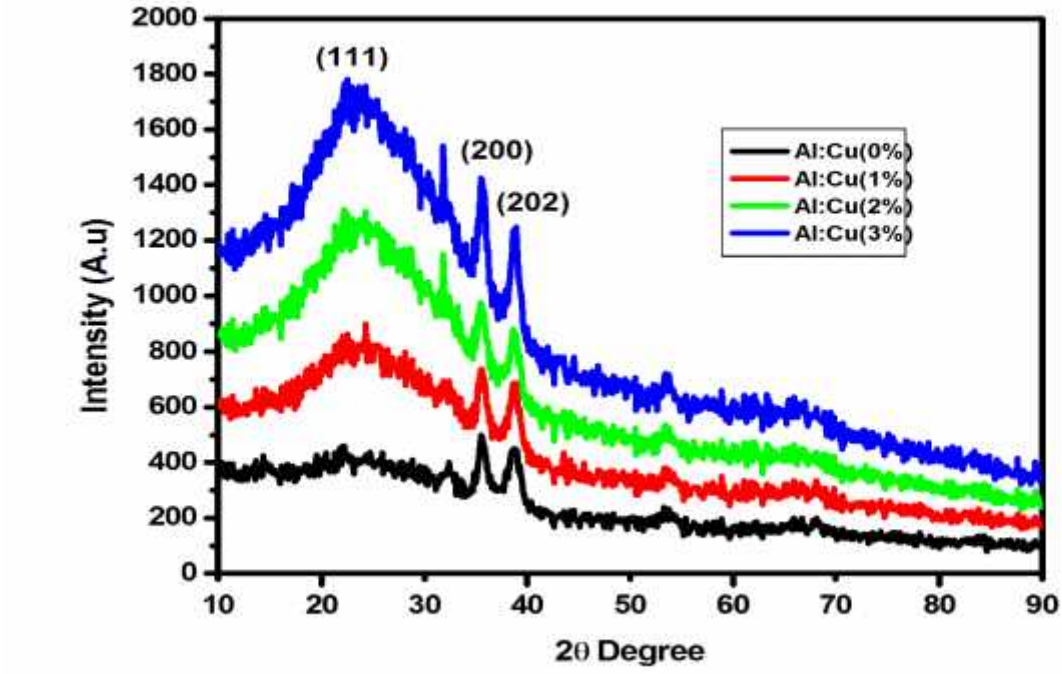

Figure-1 X-ray diffraction patterns of Al doped CuO thin film deposited at various weight percentages

$$D = \frac{0.9\lambda}{\beta cos\theta} \qquad (1)$$

Where D is the crystallite size,λis the wavelength, β is the full width at half maximum of diffraction peak measured in radians and θ is the Bragg's angle. The crystallite size calculated for the (200) plane for different Al doping concentrations are presented in Table 2. The variation in crystallite size is not well consistent with the dopant percentage and his behaviour implies that there is no direct correlation with aluminium concentration. Since crystallite size associates with several physical parameters such as, substrate temperature, spray rate, growth atmosphere, concentration of the solutions etc., it is difficult to relate crystallite size with dopant concentration. Texture coefficient [$TC_{(h\ k\ l)}$] is used to quantify preferential orientation of (200) plane in CuO thin films using the well known relation (Ali Fatima et al., 2014):

$TC_{hkl} = \underline{I_{(hkl)}/I_{o(hkl)}}$

$N^{-1}\sum_n(I_{(hkl)} / I_{o(hkl)}(2)$

Where $I_{(h\ k\ l)}$ is the measured intensity and $I_{O\ (h\ k\ l)}$ is the standard intensity from JCPDS data file and N is the number of diffraction peaks. It is found that the value of the texture coefficient is>2 for all the films which mean a well aligned crystal structure. The stacking faults probability (α) is the fraction of layers undergoing stacking sequence faults in a given crystal

and therefore one fault is expected to be observed in (1/ α) layers. The existence of stacking faults gives rise to a shift in a peak position of different reflection planes with respect to ideal position of fault free films. The relation between stacking faults probability with peak shift Δ2θ is given by (Shrividhya.T et al., 2014):

$$\alpha = \left[\frac{2\pi^2}{45\sqrt{3}}\right]\left[\frac{\Delta(2\theta)}{tan\theta}\right] \quad (3)$$

The value α is lower for 1 and 2 % Al doped CuO thin films which indicates that these films have lesser faults compared with high aluminium doped films.

Local strains (microstrain) correspond to atom displacements with respect to their positions in crystals which are free of any defects. The value of microstrain is least in undoped CuO film and the value is more pronounced for 3% Al doped CuO film (Sonmezoglu et al., 2013).

Table-1 Structural parameters of pure CuO and Al doped CuO thin films deposited various weight percentages

Percentage doping	Thickness (nm)	2θ (200) (°)	FWHM (Radian)
0	368	38.66	1.63
1	375	23.96	7.32
2	450	23.75	7.26
3	520	23.34	7.21

Table-2 Microstructural parameters of pure CuO and Al doped CuO thin films deposited at various weight percentages

Percentage doping	$D_{(Scherrer)}$ (nm)	D_{W-H} (nm)	Microstrain ($\times10^{-3}$)	Dislocation density ($\times10^{17}$) lines m^{-2}	Texture coefficient	Stacking fault probability (α)
0	5	4	0.368	4.932	1.056	0.3762
1	2	3	1.742	1.164	1.156	0.4119
2	5	6	2.728	8.453	7.654	0.4283
3	7	9	2.716	9.794	8.213	0.4281

4 MORPHOLOGICAL STUDIES

It is known that the surface property of the transparent conducting oxide films influences their optical and electrical properties which are important factors for applications of semiconductor devices. Figure 2 shows the top and cross sectional view (top-right) of SEM images Al doped CuO thin films at different various percentages. For the undoped films, uniform and very fine grains are seen on the surface and the cross sectional view gives the thickness of the film. From the SEM images, the thickness of all the samples are measured and the values range from 2 to 7 nm (Table 1). It is observed that as the doping concentration increasing in the solution of Al is larger, the thickness of the samples is found to increase which is consistent with the reported results (Helen.S.J et al., 2016). The pure CuO film shows rod shaped large grains and all the Aluminium doped films exhibit spherical shaped grains. An increase in crystallite size with 0, 1, 2 and 3% are the evidenced from SEM picture. Again, the doping concentration is found to have influence on the grain size and the agglomeration is more pronounced for films having higher dopant concentration. The disappearance of grain boundaries is well supported by the XRD result showing higher texture coefficient (8.213) for 3% Al doped CuO films.The results reveal that increasing aluminium concentration the grain sizes and voids were decreased, which agreed with the XRD result.

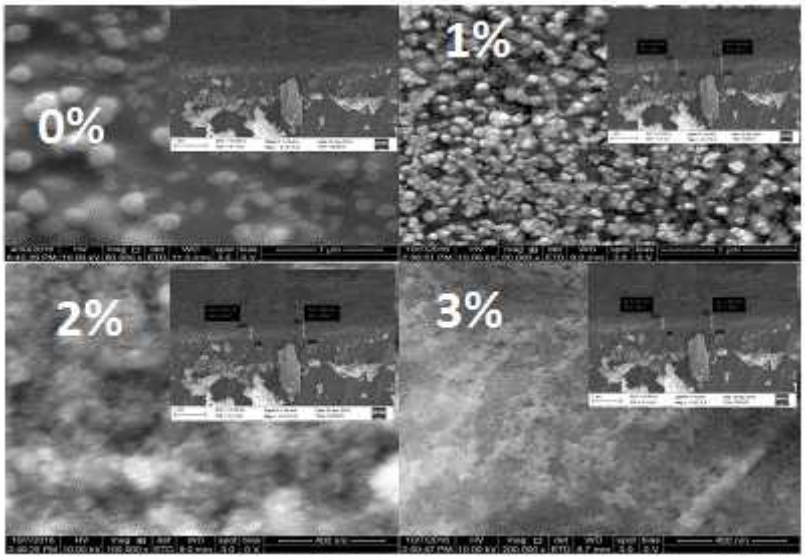

Figure-2SEM images of Al doped CuO thin films deposited at various percentages

4.1 EDAX Analysis

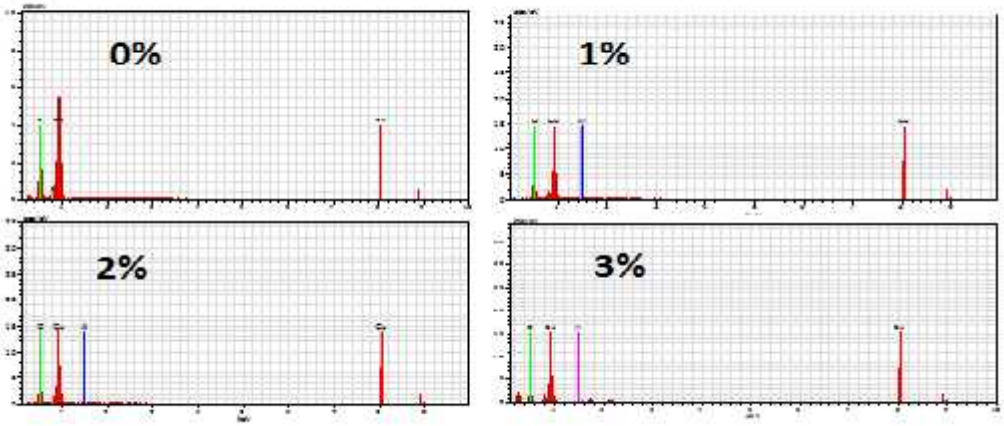

Figure-3 EDAX spectra of CuO: Al thin films 0%, 1%, 2%, 3% at 400°C

Fig 3 shows the (EDAX) Energy Dispersive X-ray analysis is one of the various versatile techniques have been used for determining that chemical composition of unknown material, by identifying the peaks in an EDAX spectrum which is that unique to an atom and therefore corresponds to a single element. Fig 3 shows the EDAX spectrum of CuO: Al thin films. The Ka radiation shown in figure indicates that all the electronic transition from ranges is L-shell to K-shell. Energy Dispersive X-ray analysis are spectrum proves that a synthesize sample are composed of an Cu and Al elements by the representation of different copper and oxygen peaks. So, that the atomic percentage of Cu and Al is Cu 54.12, O 45.88, Cu 44.25, O 47.14, Al 8.61 for 1% and Cu 53.16, O 46.30, Al 0.54 for 2%, Cu 51.14, O 47.30, Al 1.56 for 3% in (Table 3). The elemental composition analysis shows that the surface of the samples was rich in copper for various weight percentages(Ravi Dhas.C et al., 2014).

Table-3 EDAX results of CuO thin film for 0.1M

S.No	Element (K)	Wt (%)	At(%)
0%	Cu O	82.41 17.59	54.12 45.88
1%	Cu O Al	74.03 19.85 6.11	44.25 47.14 8.61
2%	Cu O Al	81.73 17.92 0.35	53.16 46.30 0.54
3%	Cu O Al	80.27 18.69 1.04	51.14 47.30 1.56

5 OPTICAL STUDIES

The transmission and absorbance spectra were deposited films have been studied from transmission spectra as shown in Fig. 4 for Al doped CuO films. The optical transmittance clearly exhibits a shift in band edge due to the variation of Al concentration and the average transmittance lies in the range of 40 – 70% in the visible region. When Al doping concentration is higher, the transmittance increases due to the incorporation of more Al atoms in the lattice sites and in the interstitials positions (Kumaravel.R et al., 2010). This is evident from the thickness measured using cross sectional SEM images that there is an increase in thickness (2-7 nm) for aluminium doped spray deposited CuO films. An increase in the film growth rate may lead to non-stoichiometric films with low absorbance(Jeong.S.H et al., 2003). The value of the optical bandgap could be calculated using the fundamental transmission which corresponds to electron excitation from the valence band to the conduction band. The absorption coefficient α and incident photon energy (hυ) are related by the Eq. (4) (Shinde.V.R et al., 2006):

$$\alpha h\vartheta = A\,(h\vartheta - Eg) \quad (9)$$

Where A is a constant (free of photon energy), E_g is the band gap of the material and exponent n is the parameter which characterize the transition process involved. The parameter n has the value of ½ for indirect allowed transition. Tauc's plot between $(\alpha h\upsilon)^{1/2}$versus energy is plotted and the linear portion of the graph is extrapolated to meet the energy axis to determine the energy band gap (Fig. 5). The band gap values of the pure CuO film is 2.31 eV and that of 1, 2 and 3% Al doped films are found to be 2.38, 2.44 and 2.48 eV, respectively.

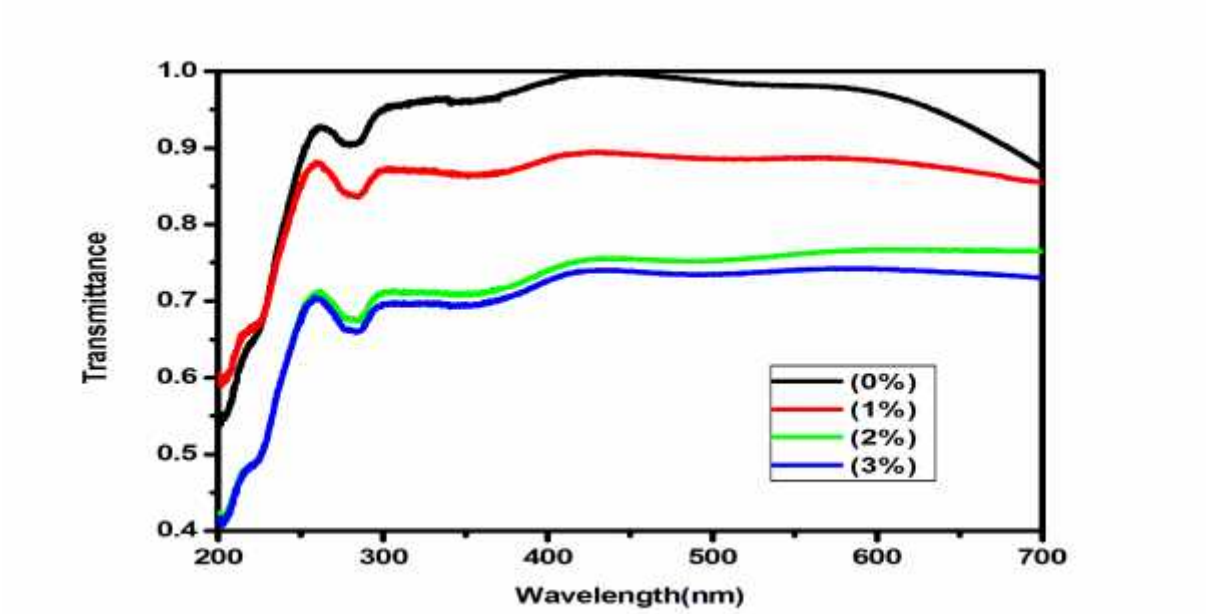

Figure-4 Transmission spectra of CuO and Al doped CuO thin films deposited at various weight percentages

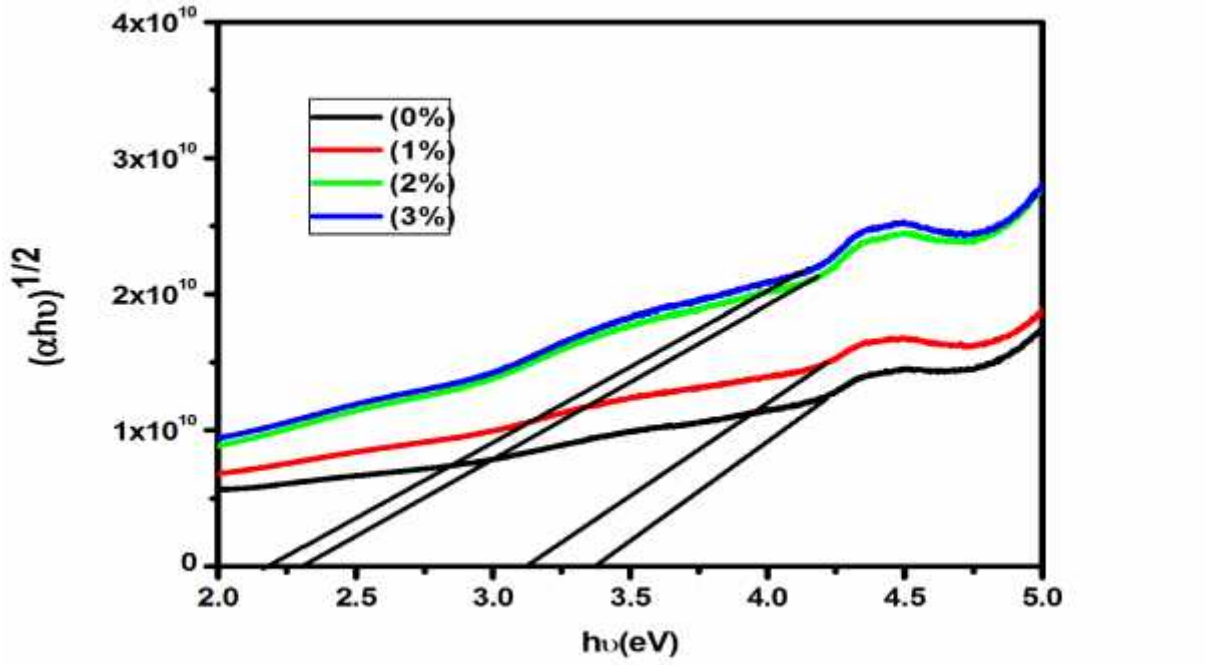

Figure-5 Optical energy band gap of CuO and Al doped CuO thin film deposited at various weight percentages

However, the energy band gap value of 3% Al doped films is blue shifted (2.79 eV) with respect to the doped film. The observed red shift in band gap may be due to the result of mutual exchange of coulomb interactions between the added free electrons in the conduction band and electron impurity scattering (Hasanzadeh.J et al., 2013, Oumous.H et al., 2001). Further the explanation for the red shift in the energy band gap values can be stated as follows: the addition of Al content into CuO creates some defects in the optical bandgap of the films and these defects produce the localized states in the optical band gap. The Al dopants may cause the changes in the localized states to overlab. Hence Al doping decreases the energy band gap of CuO films (Mou.S et al., 2014). For the observed blue shift in the band gap of 3% Al doped films can be correlated to the well known B-M energy level shift.

5.1 Photoluminescence

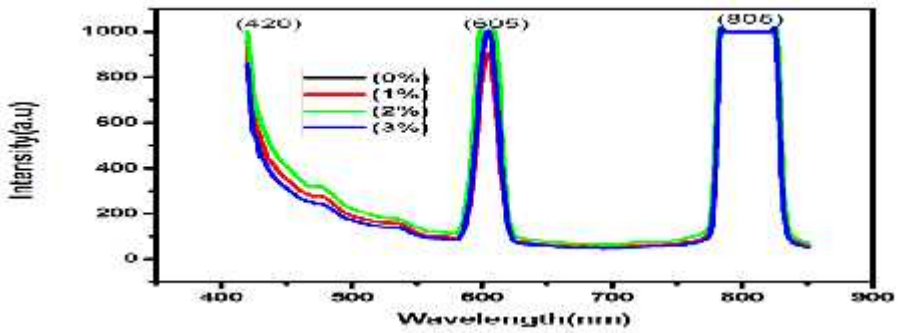

Figure-6 The PL-spectra of as-deposited Al: CuO on glass substrate at various percentages

Fig. 6 shows the photoluminescence spectra at various weight percentages of Al-doped CuO thin films. Lines at 605 nm and its second order at 805 nm are due to the semiconducting source, while peak at 420 nm corresponds to the recombination of electron and hole across the gap of CuO thin films. The wide PL band centered at 695 nm characteristic of deep levels of oxygen vacancies in the CuO matrix, and copper or oxygen atoms in interstitial position, as it was previously reported for ZnO thin films. One can note that the intensity of this wide photoluminescence band increases at 3% Al content, which can be attributed to the increase of defects in this sample(Maity.R et al., 2006).

5.2 FTIR

Fourier transform infrared (FTIR) spectroscopy is the spectroscopy that deals with the infrared region of the electromagnetic spectrum that is light with a longer wavelength and lower frequency than visible light (J.Petersen et al., 2009). The surface to volume ratio (i.e. aspect ratio) for nanoparticles is higher than their bulk counterpart. As more atoms/molecules are arranged on the surface of nanoparticle, the surface chemistry of these nanomaterials is of immense interest. In order to quickly establish the presence or absence of the various vibrational modes present in CuO: Al nanoparticle, we performed FTIR spectroscopy of CuO: Al nanoparticles. In order to analyse spectrum peaks are correlated with FTIR.

Spectroscopy correlation in Figure 7 we have FTIR spectra of as prepared nanoparticles. The absorption and transmittance bands peak obtained of CuO: Al bond and also authenticates presence of CuO: Al.

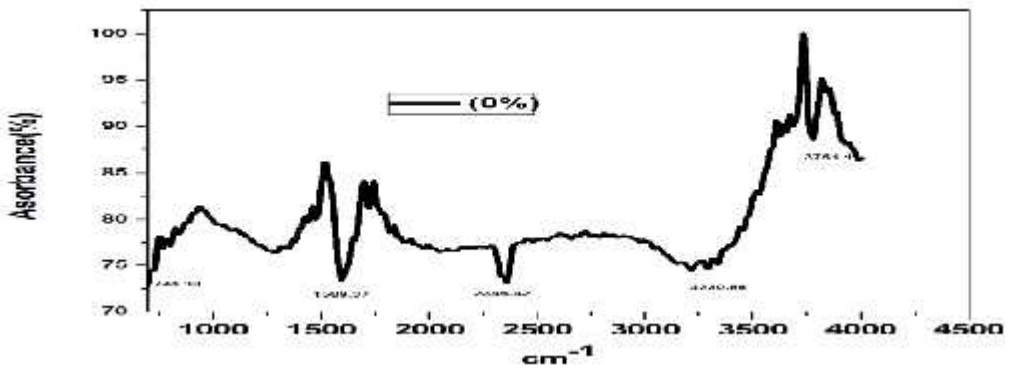

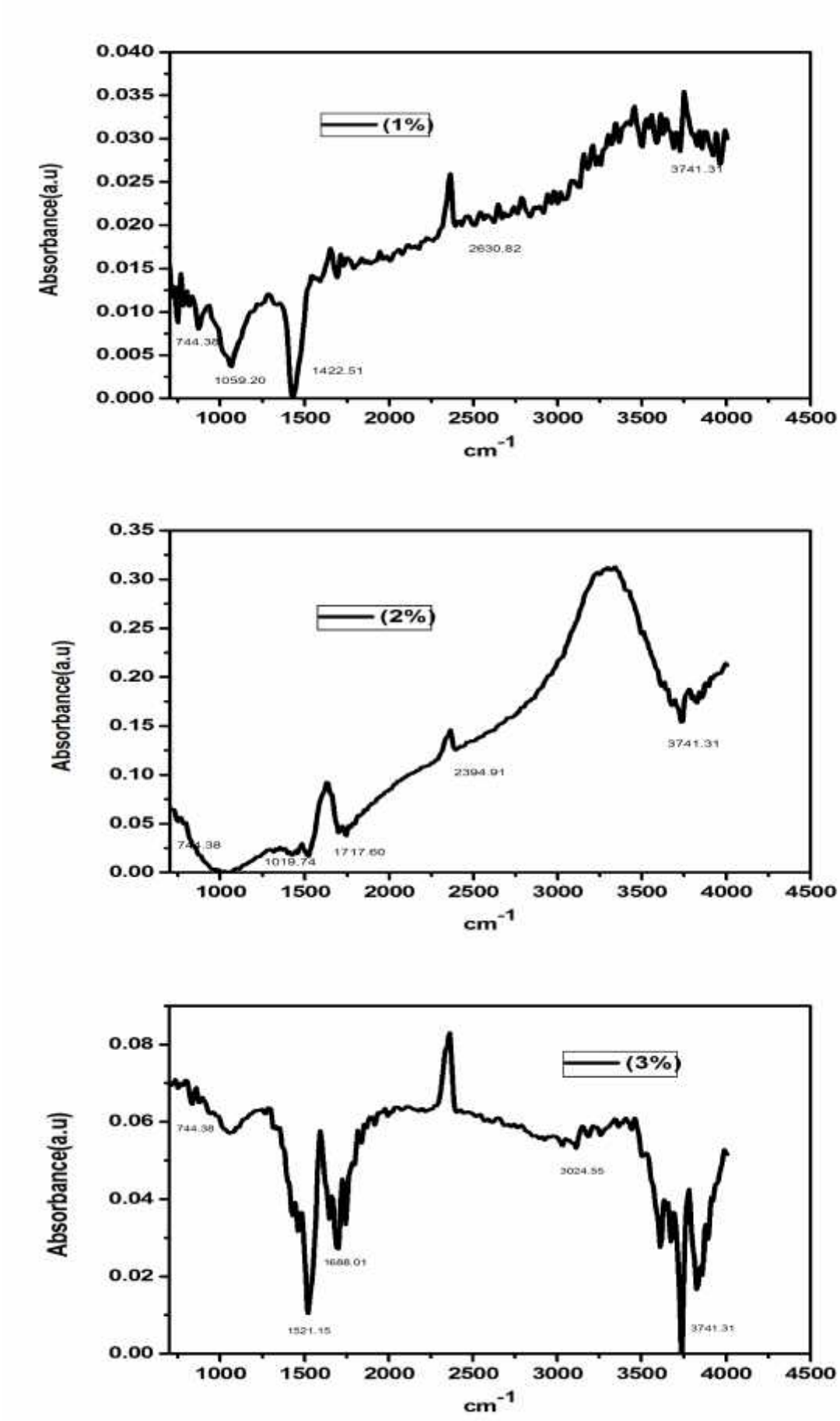

Figure-7 FTIR spectra of Al doped CuO thin film deposited at various weight percentages

6 ELECTRICAL STUDIES

The hall effect measurements of electrical properties were carried out at room temperature for Al doped CuO thin films. From the measured values, Hall coefficient (RH) were calculated for various Al-doped CuO films using the relation RH = 1/ne where e is the electronic charge. The mobility (μ) of the carriers is calculated using the relation μ = σ/ne. Fig. 6. The carrier concentration of the CuO film increases with increasing Al-doping concentration. The undoped CuO films exhibit a carrier concentration of $10.87\times10^{14}cm^{-3}$.This value increases with increasing Al-doping level and obtained by a decrease for higher doping percentage.

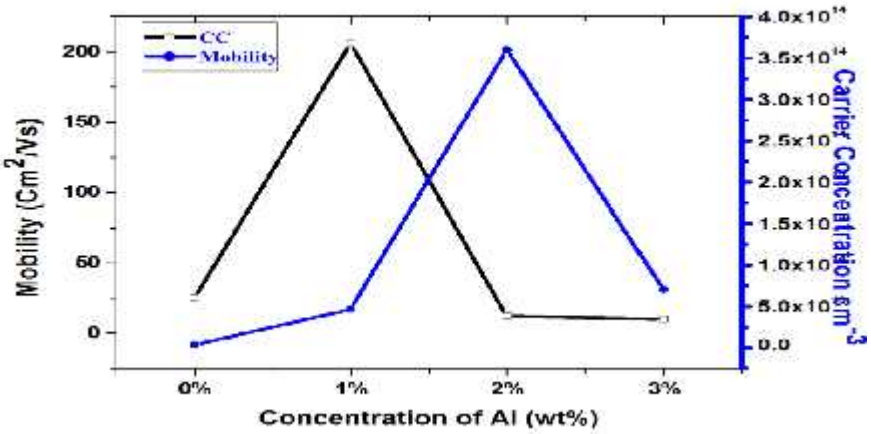

Figure-8 Mobility and carrier concentration of CuO and Al doped CuO thin films deposited at various weight percentages

The increase in carrier concentration indicates that most of the Al: CuO uniformly an effective p-type dopant rather than forming a second phase. Beyond 1% Al doping, suggesting that Al dopants are not readily ionized and some of them act as impurities in the CuO films. Mobility of the film decreases with increasing Al concentration. The undoped film shows a higher mobility of 37 cm^2Vs and it reduced to 20 cm^2Vs for the 2wt% of Al doping. A similar behaviour has been observed by (Maity.R and Chattopadhyay.K.K and Saha et al., 2007). Further, the mobility of the CuO film increases for 3wt% Al doping. The same trend has been observed for 0, 1, 2 and 3%Al doped CuO films prepared by rf sputtering method.

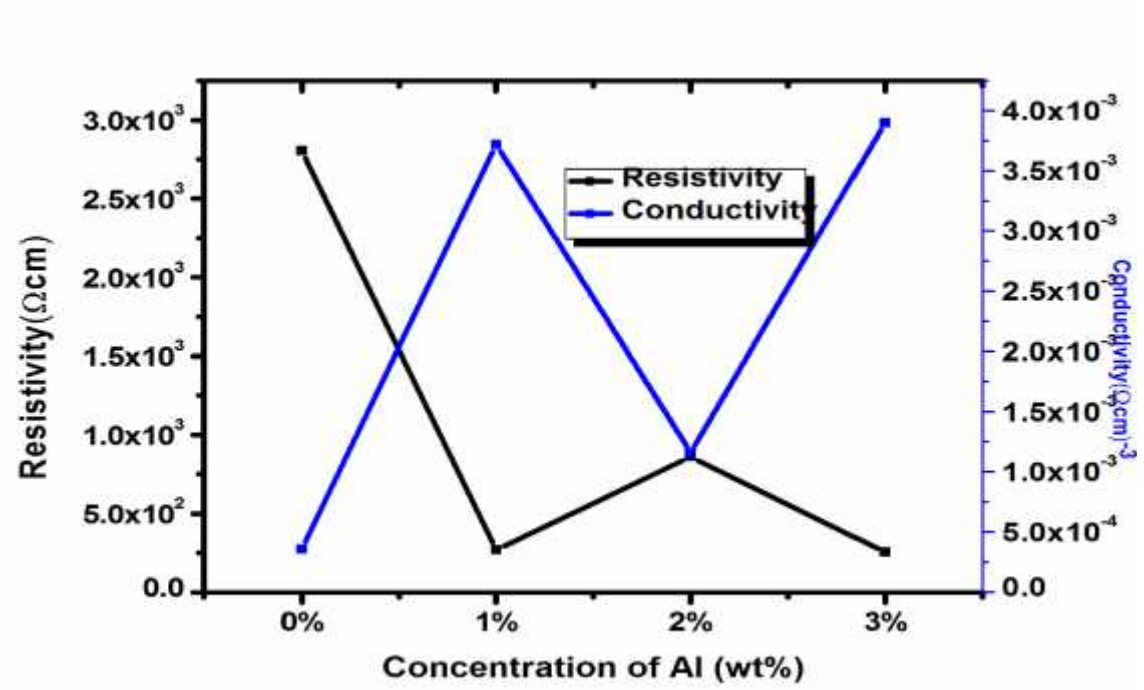

Figure-9 Resistivity and conductivity of CuO and Al doped CuO thin films deposited at various weight percentages

The variation of resistivity with Al-doping concentration is shown in Fig. 7. From the figure one can observe that the resistivity of the films was found to decrease with increasing Al-doping concentration. The undoped film has the resistivity of 3.8×10^{-3} Ωcm, the doping reduces the resistivity to 2.7×10^{3} Ωcm for 3wt% Al doping. The obtained value is lower than the Al doped copper oxide thin films prepared by rf sputtering and sol-gel method [28, 29] and are compared with other TCO materials are presented. For higher doping level the resistivity of the film increased to 2.03×10^{-4} Ωcm. The decrease in the resistivity is due to the increase in the Al-doping concentration which results in increasing free charge carrier concentration.

6.1 ANTIBACTERIAL ACTIVITY

Preparation of Test Solution and Disc

The test solution was prepared with known weight of fractions in 10 mg/mL, dissolved in 5 % Dimethyl Sulphoxide (DMSO). Sterile 6 mm discs (Himedia Ltd.) were impregnated with 20 µl of CuO and Al-doped CuO (corresponding to 100, 200 and 300 mg/mL concentations) and then allowed to dry at room temperature.

Disc Diffusion Method

The agar well diffusion method was performed by following the method (Bauer.A.W et al., 1996).Briefly, Mueller–Hinton Agar plates were prepared and 0.1 mL of standardized inoculums (0.5 O.D)was uniformly spread using a sterile cotton swab. The excess inoculums were drained and the plates were allowed to dry for 5 min. After drying, the discs with CuO and Al-doped CuO were placed on the surface of the plate with sterile forceps and gently pressed to ensure contact with the agar surface. The inoculated plates were incubated at 37 °C for 24 h. The zone of inhibition was measured and tabulated.

Table-4 Antibacterial activity of CuO and AI doped CuO against the test pathogens.

Test Pathogens	Zone of Inhibition (mm)	
	CuO	Al doped CuO
Bacillus subtilis	18	11
ETEC	12	15
Proteus mirablis	15	14
Pseudomonas aeruginosa	13	15
Staphylococcus aureus	12	14
Vibrio cholerae	10	15

A table 4 represents the antibacterial activity of pure CuO and Al-doped CuO films. The antibacterial activity of pure CuO in different concentrations against bacteria (B. subtilis, ETEC, Proteus mirabilis, Pseudomonas aeruginosa, Staphylococcus aureus, Vibrio cholerae) is observed. The antibacterial activity was determined based on an inhibition zone. No zone of inhibition was observed for the negative control. The highest mean zone of inhibition (20 mm) is recorded for pure CuO against B. subtilis (18 mm), followed by Proteus mirabilis (15 mm), S. aureus and V. cholerae (12 and 10 mm) in Table 4 which clearly indicates the antibacterial activity of the CuO. According to (Thomas D et al., 2014) CuO destroys the outer of the bacteria leading to bactericidal effect. The observed difference in the diameter of the inhibition zone may be due to the difference in the susceptibility of the different bacteria to the prepared CuO particles (Bindu.M.R et al., 2015). Table 4 reveals that the moderate effect of antibacterial activity against B. subtilis (300 mg/mL) and Proteus mirabilis (200 mg/mL and 300 mg/mL) can be attributed to the weak attachment of CuO particles towards the cell wall membrane of the bacteria resulting in the minimization of the formation of the reactive oxygen species (ROS) such as H_2O_2 which are responsible for the inhibition of the building elements of the bacteria (Ekthammathat et al., 2014). As can be seen from Table 4, the maximum antibacterial

activity of CuO was against B. subtilis. This is because of the firm attachment of CuO particles to the outer cell wall membrane of the bacteria. After that, CuO particles begin to release oxygen species into the medium(bacteria), which will inhibit the growth of cell leading to the distortion and leakage of the cell and finally the death of the cell [33]. From Table 4, it is evident that Al-doped CuO (for all concentrations) showed antibacterial activity against all the bacteria tested. Al-doped CuO showed high sensitivity of antibacterial activity against ETEC, Pseudomonas aeruginosa and Vibrio cholerae. The mean zone of inhibition ranging between 11 and 15 mm. The highest mean zone of inhibition (15 mm) is recorded against ETEC (Table 4). The high sensitivity of ETEC may be due to the doped particles which possess the appropriate size and shape of the particles. The particles with smaller size can easily penetrate and interacts into the medium. The interacted particles get accumulated into the medium in large amount and slowly affect the growth of the bacteria which leads to the death of the bacteria(Ragupathi.K.R et al., 2011). Have reported that small particles of Sn-doped CuO have a tendency to slow down the bacterial growth. Similar behaviour was observed in the present study which is due to the decreased particle size with the increase in Al concentration. During the interaction of the particle with the surface of the cell wall membrane of the bacteria, the generation of oxygen species takes place on the surface. This leads to the cleavage and elongation of the cell wall resulting from the hindering of the growth and multiplication of building elements such as DNA. The increased liberation of CuO from matrix due to the substitution of Al plays a major role in the mechanism of antibacterial activity by producing reactive oxygen species. This reactive oxygen species can kill the bacteria directly by penetrating the membrane.

7 CONCLUSION

Influence of aluminium doping in spray pyrolysed Al: CuO thin films on structural, optical and electrical properties were studied. The films show polycrystalline nature face centered cubic structure and (111) plane is the predominant peak compared with other planes. From cross sectional SEM images, it was evident that higher aluminium dopant concentration resulted in thicker films. Uniform and agglomerated grains were seen in the morphology of the films. Transmittance diminished with increase in aluminium dopant concentration while the optical absorption edge is red shifted. The FTIR result also predict the presence of Copper Oxide. From Hall effect measurements, it is found that the charge carrier concentration and mobility increases on Al doping. Antibacterial activity results indicated that 5 at.% of Al-doped CuO yielded the high antibacterial effect and potential in reducing bacterial growth for practical applications.

ACKNOWLEDGEMENT

The authors are grateful to Karunya University for providing all the necessary help for fabrication and characterization of samples. The authors are thankful to Dr.R.Ramesh Babu, Assistant Professor, School of Physics, Bharathidasan University, Tiruchirappalli-24, for extending the Hall measurement facilities established under the DST Grant (D.O.No.SR/S2/CMP-35/2004).

REFERENCES

1. Akyuz.I,Kose.S,Atay.F,Bilgin.V, 2010. Mater. Sci. Semicond. Process.13,109-111.

2. Ali Fatima.A, Devadason.S, Mahalingam.T,2014. J. Mater. Sci. Mater. Electron. 25, 3466.

3. Bhosale.C.H,Kambale.A.V,Kokate.A.V,Rajpure.K.V,2005. Mater. Sci. Eng. B 122, 67.

4. Bindu MR, Umadevi M (2015) Antibacterial and catalytic activities of green synthesized silver nanoparticles. Spectrochim Acta Part A Mol Biomol Spectrosc 135:373-378.

5. Bauer AW, Kirby WMM, Sherris JC, Turek M (1996) Antibiotic susceptibility testing by a standardized single disc method. Am J Clin Phothol 45:493-496.

6. Ekthammathat N, Thogtem S, Thongtem T (2014) Characterization and antibacterial activity of nanostructured ZnO thin films synthesized through a hydrothermal method. Anukorn Phuruangrat Powder Technol 254:199-205.

7. Gupta.R.K,Ghosh.K,Patel.R,Mishra.S.R,Kahol.P.K,2009. Curr. Appl. Phys. 9, 673.

8. HelenS.J,Suganthi Devadason and Mahalingam.T,2016.Sci,Journal of materials science: Materials in electronics 27,4426-4432.

9. Hasanzadeh.J,Taherkhani.A,Ghorbani.M, Chin.2013. J. Phys. 51, 540.

10. Houmous,Hadiri.H,2001, Thin Solid Films 386, 87.

11. Ilican.S,Caglar.M, Caglar.Y, Optoelectron,2009. Adv. Mater. Rapid Commun.3,135.

12. Jeong.S.H,Lee.J.W,Lee.S.B,Boo.J.H,2003. Thin Solid Films 435, 78.

13. Kim B, Ok YW, Shanthini TY, Ashrafi ABMA, Kumano H, Suemune I, 2003.J Crystal Growth 253,252:219.

14. Kumaravel.R, Menaaka.S, Snega.S.R.M,Ramamurthi.K,Jeganathan.K,2010. Mater.Chem. Phys. 122, 444.

15. Kumaravel.R,Bhuvaneswari.S,Ramamurthi.K,Krishnakumar.V,2012. Appl. Phys. A 109, 579.

16. Khan.M.K.R,Azizar-Rahman.M, Shahjahan.M, Mozibur-Kumaravel.R,Ramamurthi.K,Krishnakumar.V,2010. J. Phys. Chem. Solids 71, 1545.

17. MetzA.W,IrelandJ.R.,Zheng.J.G,Lobo.RP.S.M,Yang.Y,Ni.J,Stern.CL.,Dravid.V.P, Bontemps.N,Kannewurf.C.R,Poeppelmier.K.R,Marks.T.J,2004. J. Am. Chem. Soc. 126, 8477-8492.

18. Murali.K.R,Kalaivanan.A,Perumal.S,Pillai.N,2010. J. Alloys Compd. 503, 350.

19. Mane.S,Lokhande.C.D,2000. Mater. Chem. Phys. 65, 1.

20. Mou.S,Kangxian.G,Xiao.B,2014. Superlattices Microstruc. 72.

21. Maity.R,Chaltopadhyay.K.K,2006. Sol. Energy Mater. Sol. Cells 90, 597.

22. Maity.R,Chattopadhyay.K.K,2007. Solar Energy Materials Solar Cells 163, 1692.

23. Petersen.J,Brimont.C, Gallart.M, Cregut.O, Schmerber.G,Gilliot.P, Honerlage.B,Ulhaq-Bouillet.C,Rehspringer.J.L,Leuvrey.C,Colis.S,Slaoui.A,andA. Dinia,2009. Optical properties of ZnO thin films prepared by sol-gel process, Microelectron. J., Vol. 40,pp. 239-241.

24. Reddy KTR, Shanthini G.M, Johnston D, Miles RW.2003. Thin Solid Films 253,427:397.

25. Ravi Dhas.C, Dinu Alexander,Jennifier Christy.A,Jeyadheepan.K, Moses Ezhil Raj.A and Sanjeevi Raja.C,2014. Asian journal of applied sciences 7 (8):671-684.

26. Ragupathi KR, Koodali RT, Manna AC (2011) Size dependent bacterial growth inhibition and mechanism of antibacterial activity of zinc oxide nanoparticles. Langmuir 27:4020-4028.

27. Rahman.M,Hakin.M.A,Saha.D.K,Khan.J.U,2010. Curr. Appl. Phys. 10, 790.

28. Shrividhya.T, Ravi.G,Hayakawa.Y,Mahalingam.T,2014. J. Mater. Sci. Mater. Electron. 25, 3885-3894.

29. Sonmezoglu.S,Termeli.T.A,Akin.S,Askeroglu.I,2013. J. Sol-Gel. Sci. Technol. 67, 97.

30. Shinde.V.R,Gujar.T.P,Lokhande.C.D,Mane.R.S,Han.S.H,2006. Mater. Chem. Phys. 96, 326.

31. Saha.B,Das.S,Chaltopadhyay.K.K,2007 Sol. Energy Mater. Sol. Cells 91, 1692.

32. Thomas D, Abraham J, Vattappalam SC, Augustine S, Dennis Thomas T (2014) Antibacterial activity of pure and cadmium doped ZnO thin film. Indo Am J Pharma Res 4:1612-1616.

33. Zhao Z, Morel DI., Ferekides CS.2002. Thin Solid Films 118,413:203.